Applied Catalysis B: Environmental 138–139 (2013) 373–380

Contents lists available at SciVerse ScienceDirect

Applied Catalysis B: Environmental

journal homepage: www.elsevier.com/locate/apcatb

Improved low-temperature SCR activity for Fe-BEA catalysts by H_2-pretreatment

Radka Nedyalkova, Soran Shwan, Magnus Skoglundh, Louise Olsson*

Competence Centre for Catalysis, Chalmers University of Technology, SE-41296 Göteborg, Sweden

ARTICLE INFO

Article history:
Received 21 December 2012
Received in revised form 28 February 2013
Accepted 5 March 2013
Available online 13 March 2013

Keywords:
H_2-treatment
Catalyst regeneration
Low-temperature activity
Lean NO_X reduction
NH_3-SCR
Fe-BEA
Zeolite catalyst

ABSTRACT

A series of iron-exchanged zeolite beta catalysts (0.5–4 wt.% Fe) have been prepared by incipient wetness impregnation and tested for selective catalytic reduction (SCR) of NO_X with ammonia as reductant. The catalysts were characterized using BET, NH_3-TPD and XPS before and after H_2-pretreatment at 650 °C for 5 h. The NH_3-SCR activity tests show that the samples pretreated by hydrogen exhibit higher low-temperature SCR activity compared to the fresh samples, while the high-temperature activity remains almost constant. The results clearly show that the high-temperature H_2-treatment has a significant influence on the extent of different iron species formed in the zeolite. Furthermore, H_2-treatment of hydrothermally aged samples can recover some of the initial activity, although not completely due irreversible dealumination during the ageing. By H_2-pretreatment SCR catalysts with high iron loading and high activity can be prepared.

1. Introduction

Selective catalytic reduction (SCR) by urea or ammonia (NH_3) is one of the most commonly applied technologies for abatement of nitrogen oxides (NO_X) in oxygen excess [1,2]. After the first generation SCR catalysts based on vanadia supported on titania, a second generation, based on transition metal ions in zeolite structures, has emerged as promising SCR catalysts. The zeolitic frameworks, part of the pentasil series (BEA, FER, MFI) have been extensively investigated. Metal-ion exchanged zeolites, particularly based on copper and iron, represent over 80% of the recent work on NH_3-SCR [3]. Currently, copper-zeolites offer the best low-temperature performance, while iron-zeolites demonstrate the best SCR performance at high temperatures. However, several challenges arise when using these materials in exhaust after-treatment systems for diesel and lean-burn vehicles. One of the problems is thermal deactivation due to high-temperature exposure in connection with the regeneration of the particulate filter, which usually is placed upstream the SCR catalyst [4]. On the other hand, Fe-zeolites are quite tolerant to sulfur species while the activity of Cu-zeolites may deteriorate when exposed to sulfur-containg compounds, which requires desulfation [5]. The development of improved zeolite catalysts for NH_3-SCR with high hydrothermal stability as well as good low-temperature performance is crucial.

It is well-known that both the activity and hydrothermal stability of Fe-zeolites are influenced by several parameters including (i) zeolite topology, (ii) synthesis method, (iii) amount of introduced metal and (iv) post-synthesis treatment [6]. The topology has an impact on the stabilization of cations located in the microporous system of the zeolite. In addition to the zeolite framework, the Si/Al ratio has a direct influence on the SCR activity and stability of the zeolite. A high Si/Al ratio facilitates the hydrothermal stability of the zeolite by avoiding dealumination, which is a non-reversible process and proposed to be one of the major reasons for deactivation under hydrothermal conditions [6]. The synthesis method also influences the activity and stability of metal exchanged zeolites [6–8]. However, there is no general agreement in the literature on the method that is most suitable in order to obtain highly active and stable NH_3-SCR catalysts. Several studies have suggested that to achieve high SCR activity, the amount of exchanged metal should be high and the exchange process should be carefully performed. A variety of iron species and iron oxide clusters may also exist in the catalyst with a high degree of exchange [6]. On the other hand, the intrinsic activity of different iron species in the zeolite structure may differ depending on the structure, location and electronic as well as steric environment around the active sites [7]. However, in spite of abundant studies and although some well-supported hypotheses can be made, the exact structure of the active sites for NH_3-SCR in iron-zeolites remains unclear.

* Corresponding author. Tel.: +46 31 772 4390; fax: +46 31 772 3035.
E-mail address: louise.olsson@chalmers.se (L. Olsson).

0926-3373/$ – see front matter © 2013 Elsevier B.V. All rights reserved.
http://dx.doi.org/10.1016/j.apcatb.2013.03.009

Another important parameter, which significantly can change the reactivity of the catalyst, is post-synthesis treatment [7,8]. Different pretreatment methods including exposure for H_2, CO_2, O_2 and air have been used in order to increase the activity of Fe-zeolites. High-temperature treatment in inert gas or in vacuo can induce migration of dispersed iron species with subsequent clustering and grafting [9]. Several authors have concluded that only high-temperature reductive pretreatment has a beneficial effect on the activity and stability of Fe-zeolite catalysts, especially in N_2O decomposition reactions [7,9]. Furthermore, Iwasaki et al. [10] made similar observations of the effect of hydrogen treatment of Fe-ZSM-5 for NH_3-SCR. The major reason for the promotion effect of the hydrogen-pretreatment was suggested to be breakage of iron oxide clusters into smaller units, which are stabilized by forming strong bonds to the zeolite matrix and hence do not agglomerate during reoxidation. High-temperature activation results in redispersion of iron oxide clusters and therefore higher NH_3-SCR activity. Moreover, reduction at higher temperature is usually required to dehydroxylate the iron clusters, while reduction at low temperatures results in reversible reoxidation without improvement of the activity [9]. This reductive high-temperature treatment, called reductive solid-state ion exchange (RSIE), is one of the most effective ion-exchange methods for larger ions introduced into zeolite structures because of their higher cationic charges and/or larger hydration radii. However, knowledge of the morphological and structural features of the catalyst after thermal reductive activation is the key to understand the performance of the catalyst. Remaining open questions include: (i) the nature of the various additional framework sites formed during treatment, with particular attention paid to isolated and clustered species; (ii) the redox properties of extra-framework iron ions; (iii) the size of the clustered iron species present in the zeolite channels, and (iv) the influence of iron loading and thermal treatment on these parameters.

The objective of the present study is to improve the low-temperature activity for NH_3-SCR of Fe-BEA by high-temperature H_2-pretreatment. Fe-BEA catalysts loaded with 0.5–4 wt.% Fe were prepared and the catalytic performance of the samples with respect to NO_X conversion during NH_3-SCR before and after H_2-pretreatment was studied by flow reactor experiments with the focus on correlating changes of the catalytic performance with the nature of the iron species. Furthermore, the effect of H_2-treatment of hydrothermally aged samples was studied. The samples were characterized by temperature programmed desorption of ammonia, nitrogen physisorption, X-ray photoelectron spectroscopy and UV–vis spectroscopy.

2. Experimental

2.1. Sample preparation

In this study, four different iron containing zeolite catalysts (0.5; 1; 2 and 4 wt.%) were prepared by incipient wetness impregnation (IWI) at room temperature. NH_4-BEA (Zeolyst International) with a SiO_2/Al_2O_3 molar ratio of 38 was used as starting material. The iron precursor was $Fe(NO_3)_3{\cdot}9H_2O$ (Fisher Scientific) of analytical reagent grade. First, the wet volume of the pure NH_4-BEA was measured and the required amount of iron precursor was dissolved into the same volume of distilled water. Thereafter, the iron nitrate solution was introduced drop-wise to the zeolite, followed by drying at 110 °C for 12 h. Finally, the catalyst was calcined at 450 °C for 3 h, starting at room temperature with a heating rate of 2 °C/min. The Fe catalysts and the pure BEA sample were then washcoated on cordierite monoliths with length and diameter of 20 and 22 mm, respectively. The total washcoat loading was 700 mg and boehmite (Disperal D, Sasol) was used as binder. First, a thin layer of boehmite (60 mg) was deposited on the monolith walls to facilitate the attachment of the zeolite. The sample was then dried and calcined at 500 °C for 2 h before introducing the zeolite layer. The liquid:solid weight ratio used in the slurry for zeolite washcoating was 80:20, where the liquid part contained 50% water and 50% ethanol. After reaching the desired mass of washcoat, the catalyst was finally calcined at 500 °C for 2 h. Within this study, the samples are labeled by the number showing the wt.% Fe introduced.

2.2. Catalyst characterization

The textural properties of the catalysts were measured by means of N_2 physisorption isotherms at −195 °C using an ASAP 2010 sorptometer. Before the N_2 adsorption, the sample was degassed at 200 °C under vacuum conditions for 2 h in order to remove adsorbed water from the sample.

UV–vis spectra were collected using a Cary 5000 UV–vis-NIR spectrophotometer equipped with an external DRA-2500 unit. The integrating sphere permits fast acquisition of high-quality (high-resolution, low-noise) spectra. The spectra were recorded in the 200–1500 nm wavelength range, using the appropriate baseline correction.

X-ray photoelectron spectroscopy (XPS) experiments were performed using a PerkinElmer PHI 5000C ESCA system with monochromatic Al Kα radiation and 45° take-off angle. To perform the experiment, an 1 mm × 1 mm sample was cut out from an inner channel of the monolith sample and placed on the XPS sample holder. The carbon C 1s peak at 284.6 eV was used as reference for charge correction. Deconvolution of the Fe $2p_{3/2}$ peak of the catalyst was performed by fitting a Gaussian–Lorentzian (GL) function. The Lorentzian function models the lifetime broadening (natural broadening) due to the uncertainty principle relating lifetime and energy of the ejected electrons, while the Gaussian model describes the measurement process (e.g. response from instrument, the X-ray line-shape and thermal broadening). The GL-function was fitted to the experiments. The Fe^{2+} and Fe^{3+} peaks were fixed with maximum at 710.9 and 713.8 eV, respectively. The peak positions were optimized in order to achieve the lowest standard deviation, χ^2. The Gaussian–Lorentzian ratio was fixed at 20, i.e. 80% Gaussian and 20% Lorentzian.

2.3. Activity measurements

SCR activity tests and NH_3-TPD experiments were performed for degreened samples, after high-temperature H_2-treatment and after aging. The activity of the catalysts was tested in a flow reactor consisting of a horizontal quartz tube, 800 mm long with an inner diameter of 22 mm. The heating unit consisted of a heating coil, a power supply and a Eurotherm controller. Two thermocouples were available to measure the temperature in the gas phase before the catalyst, as well as in the catalyst. The inlet gas composition was controlled by Bronkhorst mass flow controllers. To analyze the gas flow, a MKS MultiGas 2030 HS FTIR spectrometer was used. The catalysts were tested in the presence of 400 ppm NH_3, 400 ppm NO, 5% H_2O and 8% O_2 and Ar as balance at a total gas flow of 3500 ml/min, which yielded a GHSV = 30,000 h^{-1}. Before the activity tests, the catalysts were degreened at 500 °C for 2 h in 8% O_2 and 5% H_2O. For the TPD study, the samples were initially exposed to 400 ppm NH_3 at 150 °C for 40 min in the presence of 5% H_2O. After saturation, the sample was flushed with Ar and 5% H_2O for 30 min, which was followed by increasing the temperature to 500 °C at 10 °C/min while exposing the catalysts to the same gas composition. Before the H_2-pretreatment, the samples was cooled to 30 °C and flushed with 4% H_2 for 5 min in order to eliminate some of the residual O_2 and H_2O, which can act as oxidants at high temperatures. The temperature

was then slowly increased (5 °C min^{-1}) to 650 °C and kept constant for 5 h. Thereafter, the sample was flushed with Ar for 10 min at the same temperature, exposed to O_2 (8%) for another 5 h and then cooled to 150 °C in Ar and H_2O. The reason for the 5 h oxidation step was to stabilize the catalyst in oxidative environment. With this step, we avoid the transient improvement in activity, which can be observed when the gas composition is switched from reductive to oxidative environment. Thereafter, NH_3-TPD and SCR experiments were performed. For the most active sample, hydrothermal aging at 700 °C for 24 h in the presence of 5% H_2O and 8% O_2 was carried out, and NH_3-TPD and SCR experiments were performed directly after the completion of this procedure. Finally, the aged sample was treated again in H_2 and the same experiments, NH_3-TPD and NH_3-SCR were performed. This final H_2-treatment step is designated regeneration.

3. Results and discussion

3.1. Catalyst characterization

Diffuse-reflectance UV–vis spectroscopy was used to assess the nature and distribution of iron species in the zeolite for the fresh powder samples. The outcome of these measurements are presented in Fig. 1. The spectra were converted to Kubelka–Munk functions and deconvoluted to Gaussian sub bands. For all spectra, two bands in the UV region peaking at 220–225 and 270–277 nm, respectively, dominate, both related to isolated Fe^{3+} species [21,22]. Further, with increasing iron content, the bands at 345 and 410 nm become more pronounced. The bands between 300 and 400 nm are assigned to small oligomeric Fe species as Fe_xO_y whereas bands above 400 nm are related to Fe_2O_3 particles located outside the zeolite pores [21,22]. For the two samples with highest iron content, another band at 530 nm can be observed. The UV–vis results clearly indicate that the nature and distribution of the iron species change with increasing iron loading for the fresh samples. Isolated iron species dominate at low Fe loading with subsequent clustering and formation of larger iron species at higher iron content.

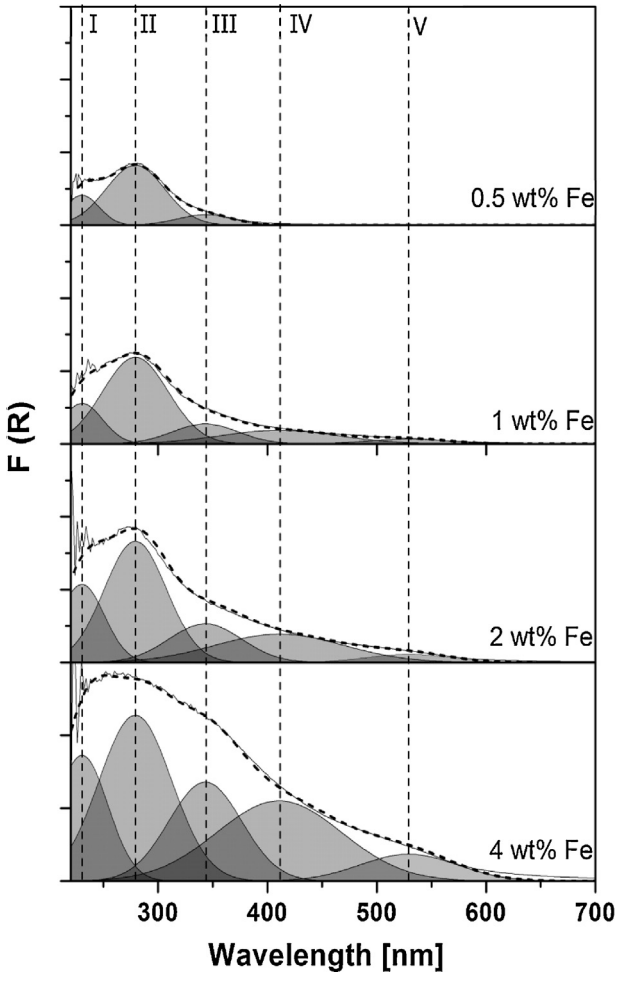

Fig. 1. UV–vis spectra of fresh Fe-BEA powder samples with 0.5, 1, 2, 4 wt.% Fe. The deconvoluted peaks for (I-II) monomeric iron species (220–290 nm), (III) dimeric and oligomeric iron species (300–400 nm) and (IV-V) larger iron oxide particles (>400 nm) are marked in the figure.

The specific surface area of the initial NH_4-BEA sample is 720 m^2/g. Introducing iron in the zeolite results in a specific surface area of 567 m^2/g washcoated monolith for the Fe-BEA sample with lowest iron loading, see Table 1. Increasing the iron loading further results in a slight decrease in the specific surface area for all samples, reaching 516 m^2/g for the sample with the highest iron loading, 4 wt.% Fe-BEA, as shown in Table 1. Since the surface area only decreased slightly with increasing iron content, these results indicate that the catalyst preparation method results in a high dispersion of iron in the cavities of the zeolite. Consistent with our results, the absence of large iron crystals for loadings up to 5 wt.% Fe, for zeolite samples prepared by the same method, was confirmed by Qi and Yang [11]. The H_2-pretreatment at 650 °C, followed by O_2-exposure at the same temperature, results in only a small decrease of the specific surface area. This implies that the microporous structure of the zeolite remains intact after H_2-treatment due to the stability of the Si—O—Si bond. These results are in line with those of Brandenberger et al. [12], showing the stability of the zeolite framework.

A good SCR catalyst should have acidic properties, which facilitate ammonia adsorption and provide sufficiently high amount of ammonia at the active SCR sites during transient conditions [3]. In this context, ammonia adsorption and desorption, in the NH_3-TPD experiments, provide information of the strength and number of acid sites in the catalyst. The data for the NH_3 uptake and desorption spectra before and after H_2-pretreatment (followed by O_2-exposure) are summarized in Table 1 and presented in Fig. 2. For the fresh and for the H_2-treated samples, the TPD spectra exhibit a broad ammonia desorption peak with a maximum between 290 and 310 °C, shown in Fig. 2. This peak is related to Brønsted acid sites in the zeolite structure. Comparing the TPD data for the fresh and for the H_2-pretreated samples, no significant shift in the peak position is observed, which indicates that no new type of sites are formed in connection with the H_2-treatment. However, the H_2-pretreatment reduces the number of Brønsted sites in all samples. Consequently, this result in lower NH_3 storage capacity for the H_2-treated compared to the fresh samples. Previously it has been found that some type of Lewis sites, related to the presence of specific kinds of extra-framework Al-species or bare ions, have different acid strength. Such types of sites are usually described as weak acid sites from which ammonia is released at relatively low temperatures [13]. From the present experiments, it can be observed that when the NH_3 supply is switched off after complete ammonia saturation for the fresh samples, the outlet NH_3 concentration decreases in the same way for all samples. For the H_2-treated samples, the NH_3 concentration after the adsorption step diminishes slower with increasing Fe content. In other words, the decreased density of the Brønsted acid sites due to the high-temperature reductive treatment is accompanied by an increased density of Lewis sites showing a clear transformation of the sites. Kustov et al. [14] have shown that Brønsted acid sites can be converted to Lewis acid sites due to dehydroxylation of the zeolite. Based on spectroscopic characterization, it was concluded that high-temperature reductive treatment results in formation of an extra-framework Fe^{2+} species

Table 1
Specific surface area, ammonia adsorption–desorption characteristics, and relative amount of Fe^{2+} for the fresh and H_2-pretreated H-BEA and Fe-BEA samples.

Samples[a]	BET[b], m^2/g	NH_3 ads[b,c], mmol/g	NH_3 weak[b], mmol/g	NH_3 des[b], mmol/g	$\frac{Fe^{2+}}{(Fe^{2+}+Fe^{3+})}$ [%]
H-BEA – F	–	0.958	0.293	0.665	–
H-BEA – H_2	–	0.942	0.292	0.650	–
0.5 wt.% Fe-BEA – F	567	0.972	0.308	0.664	63
0.5 wt.% Fe-BEA – H_2	565	0.895	0.325	0.570	69
1 wt.% Fe-BEA – F	562	0.976	0.309	0.667	63
1 wt.% Fe-BEA – H_2	559	0.936	0.364	0.572	82
2 wt.% Fe-BEA – F	533	0.981	0.325	0.656	59
2 wt.% Fe-BEA – H_2	500	0.960	0.405	0.555	84
4 wt.% Fe-BEA – F	516	0.988	0.340	0.648	75
4 wt.% Fe-BEA – H_2	469	0.990	0.430	0.560	87

[a] *F* = fresh, H_2 = H_2-pretreated.
[b] Sample weight includes the mass of the monolith and the washcoat.
[c] Total NH_3 ads = NH_3 weak + NH_3 des.

and simultaneous redispersion of iron oxide clusters [9,15,16]. The extraction of the heteroatom to extra-framework positions causes a decrease in the number of Brønsted acid sites in agreement with our TPD results. The more severe reductive treatment suggested by other authors results in the formation of extra-framework Fe—O—Al species [17]. Pirngruber et al. [9] tried to identify such Fe—O—Al bonds using EXAFS for samples reduced at 600 °C. The EXAFS spectra were fitted with a mixed backscattering by Fe and Al, but the two shells were strongly correlated. Consequently, the EXAFS analysis could not provide proof of the formation of Fe—O—Al clusters. Furthermore, Amunziata et al. [18] studied Fe-ZSM-5 as NH_3-SCR catalyst and concluded that the NO_X conversion appears to be a function of the amount of Fe^{2+} species in the catalysts. Based on the results mentioned above, we suggest that the presence of Fe^{2+} might promote the NH_3-SCR reaction, especially at low temperatures. Our findings provide new data for the discussion of the type of Fe species responsible to SCR of NO_X.

X-ray photoelectron spectroscopy is a versatile surface analysis technique that may be used to qualitatively determine the oxidation states of iron. Fig. 3 shows the Fe $2p_{3/2}$ spectra for both fresh and H_2-treated samples. Two distinct bands centered at 710.9 and 713.8 eV are observed in all spectra. These values are close to the range of Fe $2p_{3/2}$ binding energies of iron in FeO and Fe_2O_3 [19,20] respectively, indicating that the iron in our samples is present both as Fe^{2+} and Fe^{3+}. Fig. 3 also shows the deconvoluted Fe $2p_{3/2}$ peak for all samples. The experimental data are shown as thin gray solid lines, while the fitted peaks, attributed to Fe^{2+} and Fe^{3+}, are shown as solid black lines. The peak areas for Fe^{2+} and Fe^{3+} are marked by

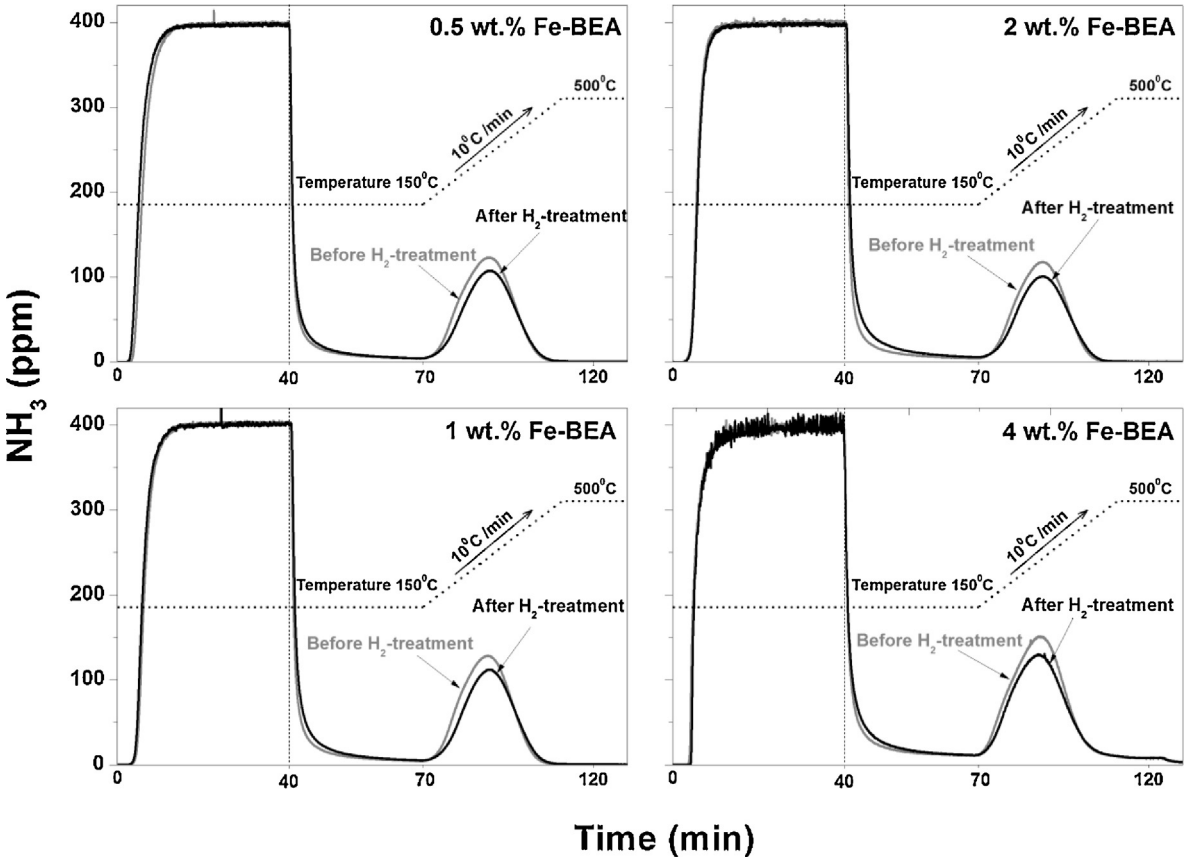

Fig. 2. NH_3 uptake and desorption spectra for the studied Fe-BEA catalysts with 0.5–4 wt.% Fe. Grey lines show the data before H_2-pretreatment and black lines show the data after H_2-pretreatment. The samples are exposed to 400 ppm NH_3 and 5% H_2O for 40 min at 150 °C, followed by 30 min Ar and 5% H_2O flowing over the catalyst and finally a temperature ramp of 10 °C/min to 500 °C is applied. The total flow rate is 3500 ml/min.

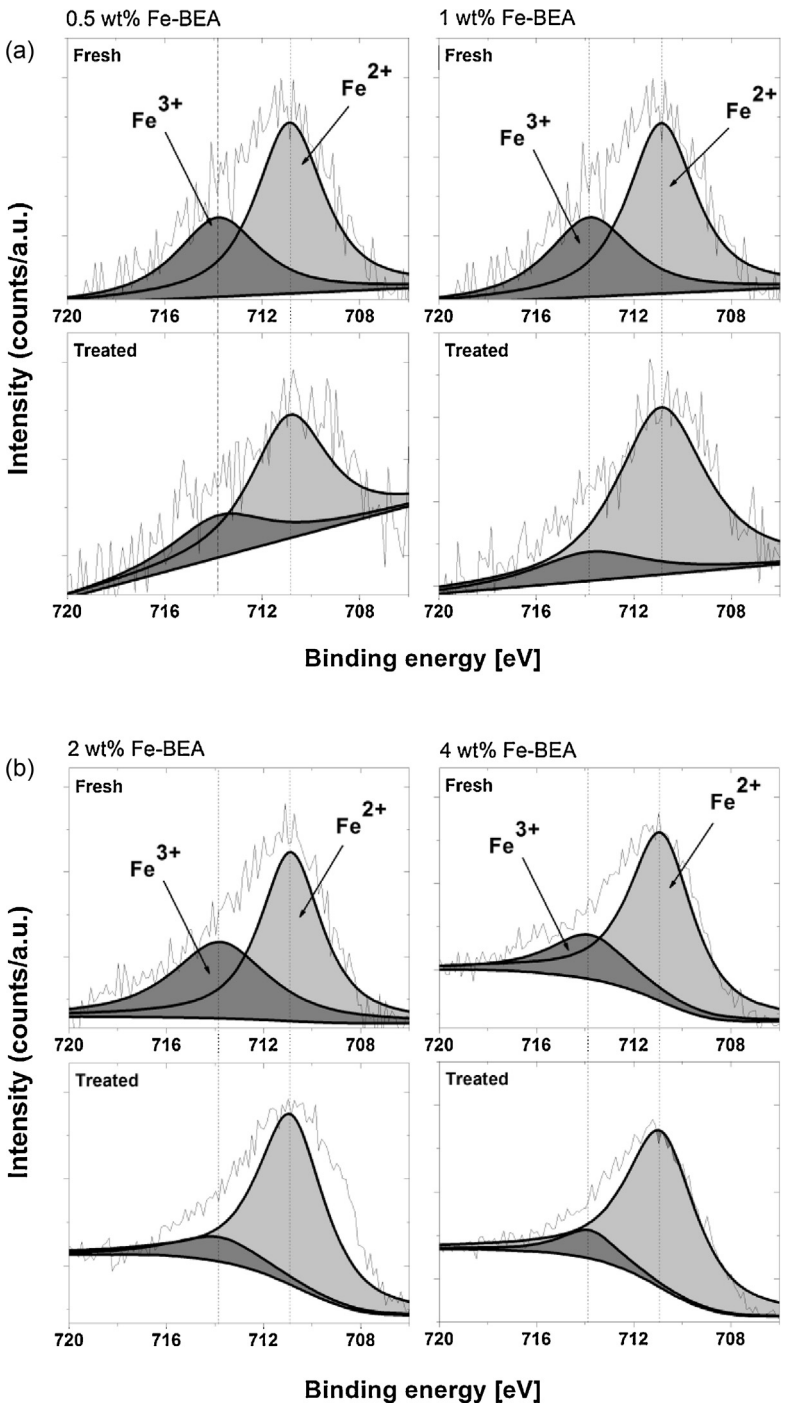

Fig. 3. Deconvolution of the Fe $2p_{3/2}$ XPS peak for the studied catalysts before and after H_2-pretreatment. The deconvoluted peaks are marked with Fe^{3+} and Fe^{2+} respectively. (a) Results for the Fe-BEA samples with 0.5 and 1 wt.% Fe, and (b) with 2 and 4 wt.% Fe.

dark and light gray, respectively. In Table 1, the ratio between the peak areas for Fe^{2+} and the sum of Fe^{2+} and Fe^{3+} for the samples is summarized.

The data show that the H_2-pretreatment results in increased relative Fe^{2+} concentration in all samples. On the other hand, as the Fe loading increases, the difference in the relative amount of Fe^{2+} before and after H_2-treatment continuously increases, starting from 6% for the 0.5 wt.% Fe-BEA sample to 25% for the 2 wt.% Fe-BEA sample. However, for the 4 wt.% Fe-BEA sample, the H_2-pretreatment results in 12% higher relative amount of Fe^{2+}. The explanation for this phenomenon might be related to the fact that as the iron loading increases, larger iron clusters are formed in the fresh catalyst and the redox ability of such clusters is considerably lower compared to smaller iron species. This results in only a limited quantity of Fe reduced by the H_2-pretreatment. Despite the lower transformation to Fe^{2+} species after H_2-pretreatment for the 4 wt.% Fe-BEA sample, the quantity of Fe^{2+} is still the highest in this sample.

3.2. Catalytic activity

The results for the NH_3-SCR experiments are shown in Fig. 4. For all iron loadings, the fresh and the H_2-treated samples are compared. At 150 °C the samples exhibit no SCR activity. However,

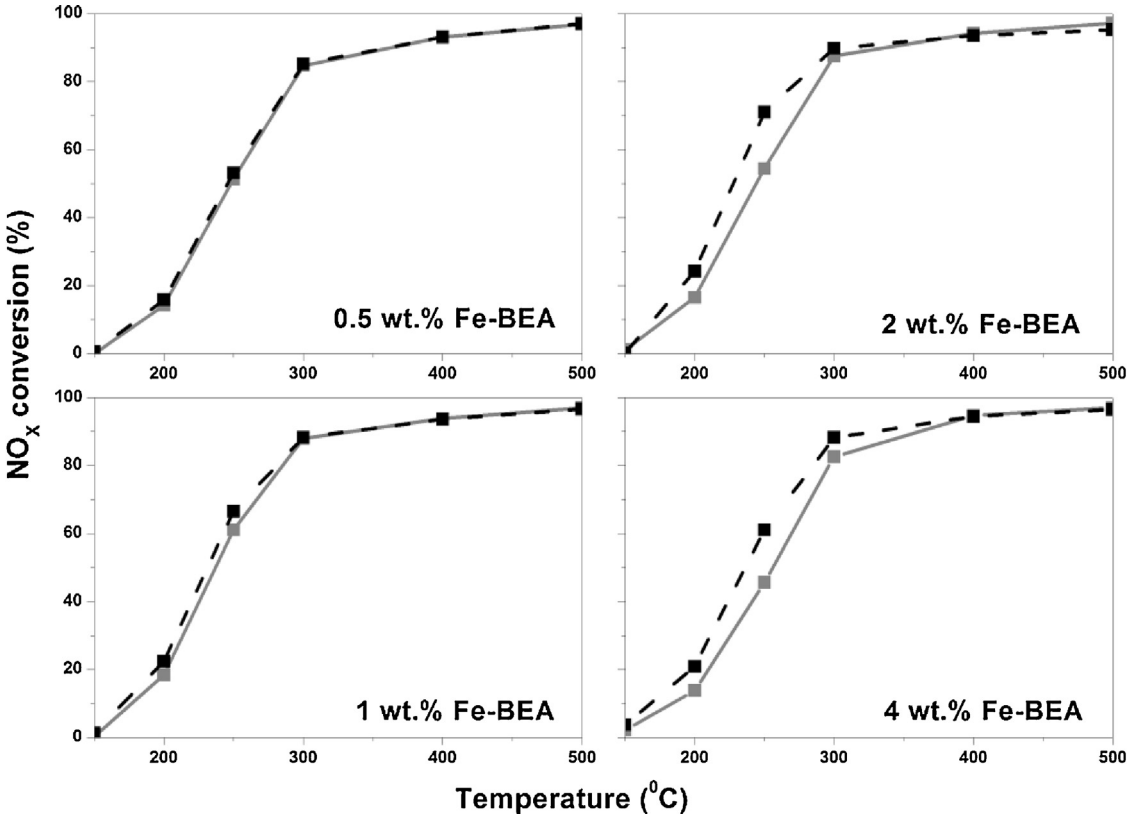

Fig. 4. NO_X conversion during NH_3-SCR over Fe-BEA catalysts with 0.5–4 wt.% Fe. Solid grey lines show the activity before H_2-pretreatment and dashed black lines show the activity after H_2-pretreatment. The samples were exposed to 400 ppm NO, 400 ppm NH_3, 8% O_2 and 5% H_2O and the temperature was increased stepwise from 150 to 500 °C.

above 150 °C the activity increases with increasing temperature. It can clearly be seen that high-temperature H_2-pretreatment results in improved NO_X conversion, especially in the lower temperature region (200–300 °C). At higher temperatures (>300 °C), all catalysts exhibit similar increase of the SCR activity. In addition, the difference in NO_X conversion before and after H_2-pretreatment is more pronounced with increasing iron loading. For the 0.5 wt.% Fe-BEA sample, the NO_X conversion increases by 2–3 percentage units at 250 °C, while for the 2 wt.% Fe-BEA sample the NO_X conversion increases by up to 18 percentage units at the same temperature. A similar value was obtained for the 4 wt.% Fe-BEA sample. The 1 wt.% Fe-BEA sample is the most active catalyst before the H_2-treatment, whereas the 2 wt.% Fe-BEA sample offers the best performance after the treatment. As the results from the XPS experiments show that Fe mainly is present in a divalent state after H_2-treatment and that the relative Fe^{2+} concentration progressively increases, it is reasonable to expect better SCR performance for the 4 wt.% Fe-BEA sample in comparison with the 2 wt.% Fe-BEA sample. However, the NO_X conversion for the 4 wt.% Fe-BEA sample is lower compared to that of the 2 wt.% Fe-BEA sample. The lower activity for the former sample is probably due to the coexistence of species with higher nuclearity. The catalytic data shows that the activity mainly is a function of the distribution of iron species, a consequence of the Fe content and the H_2-pretreatment [6].

Devadas et al. [24] suggested that NO oxidation over Fe_2O_3 particles in the zeolite is the rate-determining step for the NH_3-SCR reaction over Fe–ZSM-5. One widely accepted hypothesis is that the active sites for selective reduction of NO with NH_3 are isolated Fe^{2+} species in close vicinity to the Al^{3+} framework. In our previous studies [25,26,30], the NH_3-SCR experiments for hydrothermally aged samples show lower activity for NO reduction below 300 °C compared to the corresponding fresh samples, whereas the activity for NO oxidation is higher and observed already at 150 °C. When comparing the results from the NO oxidation and NH_3-SCR experiments, the increased oxidation of NO does not result in increased NH_3-SCR activity at lower temperatures. Our results demonstrate that the low-temperature NO reduction is dependent on the Fe^{2+}/Fe^{3+}-ratio. Tronconi and co-workers [27] confirmed the corresponding dynamics of Fe species in the reaction pathway and emphasized the cooperative interaction between the zeolitic acid sites, where the ammonia is stored, and the iron red-ox sites of the catalyst, which are involved in the critical reduction of the surface nitrates by NO. Based on spectroscopic studies, Rivallan et al. [28] showed that NO interacts with isolated Fe^{2+} centers in formation of tri-nitrosylic and di-nitrosylic complexes, while Fe^{3+} forms only a mono-nitrosylic complex. The difference in the capability of Fe^{2+} and Fe^{3+} to interact with NO and further react with stored ammonia might be another factor for NH_3-SCR activity at low temperatures. Comparing the vibration frequencies of the nitrosylic Fe^{2+} complexes for samples with and without introduction of extra aluminum (to the zeolite) Rivallan et al. [28] concluded that the Al is located close to Fe sites. Further, the intensity of the NO peaks was higher for the samples containing extra Al. This means that Al promotes high Fe dispersion and hence increases the abundance of mononuclear or low-nuclearity Fe species. Discussing the active sites in the NH_3-SCR reaction, Al vicinity is another parameter to be considered due to promoting iron dispersion.

The most active catalysts after H_2-pretreatment in the present investigation is the 2 wt.% Fe-BEA sample which further was subjected to a hydrothermal stability test at 700 °C in 5% H_2O and 8% O_2 for 24 h. The NO_X conversions from the NH_3-SCR experiments after the different pretreatments are compared in Fig. 5. As mentioned above, the NO_X conversion at 250 °C for the 2 wt.% Fe-BEA sample increases from 54 to 71% after H_2-pretreatment. After hydrothermal aging, the NO_X conversion decreases and reaches

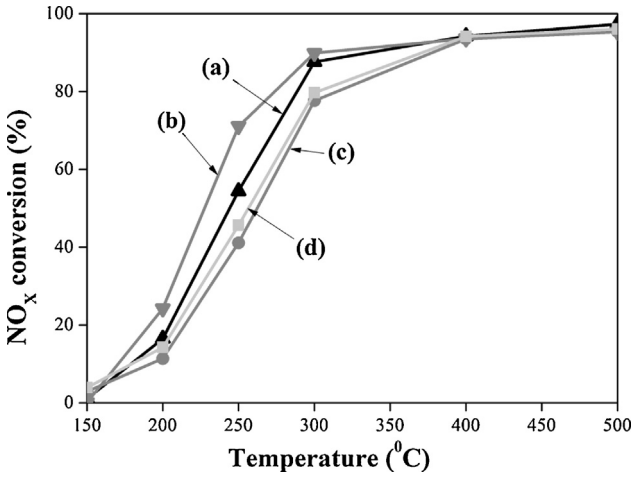

Fig. 5. NO_X conversion during NH_3-SCR for the 2 wt.% Fe-BEA sample after different pretreatment conditions: (a) ▲ – fresh sample; (b) ▼ – after H_2-pretreatment; (c) ● – after hydrothermal aging at 700 °C for 24 h; (d) ■ – after H_2-treatment of the aged sample referred as regeneration. The samples were exposed to 400 ppm NO, 400 ppm NH_3, 8% O_2 and 5% H_2O and the temperature was stepwise increased from 150 to 500 °C.

40% at 250 °C. However, the H_2-treatment of the aged 2 wt.% Fe-BEA sample results in increased NO_X conversion to 45% at 250 °C, although lower compared to the fresh catalyst. The data reported in Fig. 5 show that the H_2-treatment does not prevent the catalyst from further deactivation. It is possible that dealumation occurs simultaneously, which is a parallel non-reversible deactivation process that could be the main reason for the lower NO_X conversion after aging [6]. Furthermore, in a recent study of 1 wt.% Fe-BEA using DRIFT spectroscopy [29] it was shown that oligomeric iron clusters are formed in the zeolite pores after short time of thermal treatment due to migration of isolated iron species. Longer thermal treatment results in a continuous migration and formation of larger iron oxide particles located on the external surface of the zeolite. The improved NH_3-SCR activity due to H_2-treatment after ageing is most likely related to redispersion of oligomeric iron clusters in the zeolite pores and not to redispersion of iron particles on the surface of the zeolite crystals. Pérez-Ramírez at al. [23] studied the same type of catalyst, Fe-BEA after reduction in H_2/Ar flow by means of UV–vis spectroscopy. The authors observed a decrease in band intensity due to reduction of Fe^{3+} species. However, subsequent treatment of the reduced samples in air did not completely restore the intensity of bands above 400 nm, indicating that a fraction of relatively large iron oxo-clusters and iron oxide particles remain in a reduced state after oxidative treatment. Based on the results from the characterization and activity studies in the present work, we suggest that the high-temperature reductive treatment likely causes migration of Fe^{3+} species to the extra-framework position (isolated and/or clusters) followed by reduction to Fe^{2+}. These sites are highly coordinatively unsaturated and compensate for the loss of coordinated water by forming strong bonds with the zeolite matrix without further agglomeration. The characterization techniques used in the present study clearly indicate that in the H_2-treated samples, iron is mainly present in a divalent state and the nuclearity of the iron species is a function of the iron loading.

4. Conclusions

In this study, we have prepared Fe-BEA catalysts with different iron loading (0–4 wt.%) via incipient wetness impregnation. The following order in SCR activity before H_2-treatment is established with the least active sample first: H-BEA ≪ 4 wt.% Fe-BEA < 0.5 wt.% Fe-BEA < 2 wt.% Fe-BEA < 1 wt.% Fe-BEA. However, after H_2-pretreatment of the samples, the order changes to: H-BEA ≪ 0.5 wt.% Fe-BEA < 4 wt.% Fe-BEA < 1 wt.% Fe-BEA < 2 wt.% Fe-BEA. The improvement in low-temperature activity is concluded to be due to redispersion of Fe in the zeolite structure by hydrogen. The redispersion is explained by breaking of iron oxide clusters into smaller units, which are stabilized by forming strong bonds to the zeolite matrix. The latter might also be the reason why these units do not agglomerate during reoxidation. Through this treatment, SCR catalysts with high iron loading and high activity can be prepared. The characterization techniques show that iron mainly is present in divalent oxidation state. The NH_3-TPD experiments performed before and after H_2-pretreatment show a transformation of the Brønsted acid sites into weak Lewis sites. After hydrothermal aging, the H_2-treatment does not prevent further deactivation of the catalyst, which could be due to the dealumination, a parallel non-reversible process. However, the initial activity can partially be recovered by H_2-treatment.

Acknowledgments

This work was performed at the Competence Centre for Catalysis (KCK), Chalmers University of Technology. KCK is financially supported by Chalmers, the Swedish Energy Agency and the following member companies: AB Volvo, ESCAPS AB, Haldor Topsøe A/S, Scania CV AB, Volvo Car Corporation AB. We would also like to gratefully acknowledge the Swedish Foundation for Strategic Research (F06-0006) and the Chalmers Initiative Transport for funding.

References

[1] K. Skalska, J.S. Miller, S. Ledakowicz, Science of The Total Environment 408 (2010) 3976.
[2] Z. Liu, S.I. Woo, Catalysis Reviews: Science and Engineering 48 (2006) 43.
[3] K. Kamasamudram, N.W. Currier, T. Szailer, A. Yezerets, SAE International, 2010-1-1182, 2010.
[4] B. Moden, J.M. Donohue, W.E. Cormier, H.X. Li, Topics in Catalysis 53 (2010) 1367.
[5] Y. Cheng, G. Cavataio, C. Lambert, SAE International, 2010-1-1182, 2008.
[6] S. Brandenberger, O. Kröcher, A. Tissler, R. Althoff, Catalysis Reviews: Science and Engineering 50 (2008) 492.
[7] A. Zecchina, M. Rivallan, G. Berlier, C. Lamberti, G. Ricchiardi, Physical Chemistry Chemical Physics 9 (2007) 3483.
[8] S. Branderberger, O. Kröcher, A. Tissler, R. Althoff, Industrial & Engineering Chemistry Research 50 (2011) 4308.
[9] G.D. Pirngruber, P.K. Roy, N. Weiher, Journal of Physical Chemistry B 108 (2004) 13746.
[10] M. Iwasaki, K. Yamazaki, K. Banno, H. Shinjoh, Journal of Catalysis 260 (2008) 205.
[11] G. Qi, R.T. Yang, Applied Catalysis B 60 (2005) 13.
[12] S. Brandenberger, O. Kröcher, M. Casapu, A. Tissler, R. Althoff, Applied Catalysis B 101 (2011) 649.
[13] M. Høj, M.J. Beier, J-D. Grunwaldt, S. Dahl, Applied Catalysis B 93 (2009) 166.
[14] L.M. Kustov, A.L. Tarasov, V.I. Bogdan, A.A. Tyrlov, J.W. Fulmer, Catalysis Today 61 (2000) 123.
[15] Q. Zhu, R.M. van Teeffeler, E.J.M. Hensen, Journal of Catalysis 221 (2004) 575.
[16] P.K. Roy, R. Prins, G.D. Pingruben, Applied Catalysis A-General 80 (2008) 226.
[17] A. Ates, C. Hardacre, Journal of Colloid and Interface Science 372 (2012) 130.
[18] O.A. Anunziata, A.R. Beltramone, Z. Juric, L.B. Pierella, F.G. Requejo, Applied Catalysis A 264 (2004) 93.
[19] S.J. Roosendaal, B. van Asselen, J.W. Elsenaar, A.M. Vredenberg, F. Habraken, Surface Science 442 (1999) 29.
[20] D.D. Hawn, B.M. Dekoven, Surface and Interface Analysis 10 (1987) 63.
[21] M.S. Kumar, M. Schwidder, W. Grünert, A. Brückner, Journal of Catalysis 227 (2004) 384.
[22] S. Branderberger, O. Krocher, A. Tisser, R. Althoff, Applied Catalysis A 373 (2010) 168.
[23] J. Pérez-Ramírez, J.C. Groen, A. Brückner, M.S. Kumar, U. Bentrup, M.N. Debbagh, L.A. Villaescusa, Journal of Catalysis 232 (2005) 318.
[24] M. Devadas, O. Kröcher, M. Elsener, A. Wokaun, G. Mitrikas, N. Söger, M. Pfeifer, Y. Demel, L. Mussmann, Catalysis Today 119 (2007) 137.

[25] S. Shwan, R. Nedyalkova, J. Jansson, J. Korsgren, L. Olsson, M. Skoglundh, Industrial & Engineering Chemistry Research 51 (2012) 12762.
[26] S. Shwan, J. Jansson, J. Korsgren, L. Olsson, M. Skoglundh, Catalysis Today 197 (2012) 24.
[27] M.P. Ruggeri, A. Grossale, I. Nova, E. Tronconi, H. Jirglova, Z. Sobalik, Catalysis Today 184 (2012) 107.
[28] M. Rivallan, G. Ricchiardi, S. Bordiga, A. Zecchina, Journal of Catalysis 264 (2009) 104.
[29] S. Shwan, E. Adams, J. Jansson, M. Skoglundh, Catalysis Letters 143 (2013) 43–48.
[30] S. Shwan, R. Nedyalkova, J. Jansson, J. Korsgren, L. Olsson, M. Skoglundh, Topics in Catalysis (2013), http://dx.doi.org/10.1007/s11244-013-9933-4.